Chemical Science

EDGE ARTICLE

View Article Online
View Journal | View Issue

Cite this: *Chem. Sci.*, 2016, **7**, 4140

Differential effects of zinc binding on structured and disordered regions in the multidomain STIL protein†

Hadar Amartely,[a] Ahuvit David,[bc] Mai Shamir,[a] Mario Lebendiker,[d] Shai Izraeli[bc] and Assaf Friedler*[a]

Received 10th January 2016
Accepted 1st March 2016

DOI: 10.1039/c6sc00115g

www.rsc.org/chemicalscience

Binding of metal ions is an important regulatory mechanism in proteins. Specifically, Zn^{2+} binding to disordered regions commonly induces a disorder to order transition and gain of structure or oligomerization. Here we show that simultaneous binding of Zn^{2+} ions has different effects on structured and disordered domains in the same multidomain protein. The centrosomal STIL protein bound Zn^{2+} ions *via* both its structured N-terminal domain (NTD) and disordered central region (IDR). Zn^{2+} binding induced structural rearrangement of the structured NTD but promoted oligomerization of the IDR. We suggest that by binding Zn^{2+} STIL acquires a different conformation, which allows its oligomerization and induces its activity. Sequence alignment of the oligomerization region revealed a new suggested motif, SxKxS/SxHxS/SxLxS, which may participate in STIL oligomerization. Binding of the same metal ion through a disordered and a structured domain in the same protein is a property that may have implications in regulating the protein activity. By doing so, the protein achieves two parallel outcomes: structural changes and oligomerization that can take place together. Our results describe a new important role of the delicate interplay between structure and intrinsic disorder in proteins.

Introduction

Binding of metal ions may induce structural changes in proteins as a means of regulating protein activity.[1–3] Metal ions can also play a role in protein oligomerization.[4–6] Binding of metal ions to disordered proteins may induce a disorder-to-order transition, stabilizing the active conformation and enabling the protein to function.[7–9] Metal binding can also induce oligomerization of a disordered protein.[10–12] Here we show that the binding of Zn^{2+} ions may have different effects on structured and disordered domains in the same multidomain protein. Our model protein in this study is STIL (SCL/TAL1 Interrupting Locus) which is a 150 kDa cytosolic protein that contains 1288 residues.[13] STIL plays an essential role in cell proliferation and survival[14–16] and is required for centrosomal biogenesis and centriolar duplication.[17–19] STIL has two functional orthologue proteins, *Drosophila* ANA-2 and *C. elegans* SAS-5. Both are centrosomal proteins that play a role in centriolar assembly.[20,21] STIL is involved in several types of cancer[14,22] and in autosomal recessive primary microcephaly.[23] We have previously shown that STIL contains an intrinsically disordered central region that mediates its protein interactions.[24–26] In addition, it contains a structured N-terminal domain, a short coiled coil domain and a STAN motif[27] (Fig. 1A). STIL was also shown to oligomerize.[21,26,28] The STIL orthologues ANA-2 and SAS-5 also form oligomers and SAS-5 contains an intrinsically

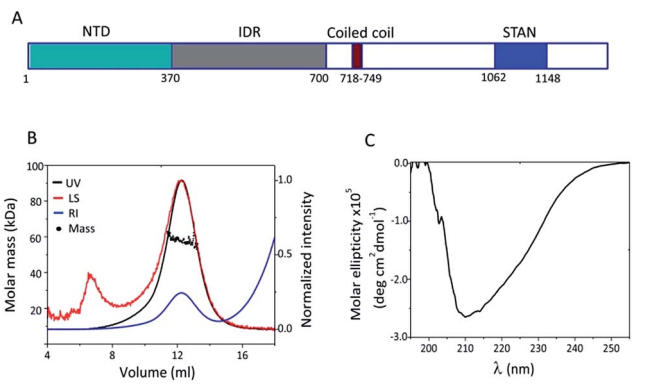

Fig. 1 Structural characterization of STIL NTD: (A) a schematic illustration of the STIL domains. (B) SEC-MALS chromatogram of HLT STIL NTD – the protein is a monomer. (C) CD spectrum of HLT STIL NTD – the protein is mainly structured.

[a]*Institute of Chemistry, Hebrew University of Jerusalem, Safra Campus, Givat Ram, Jerusalem 91904, Israel*

[b]*Sheba Cancer Research Center and the Edmond and Lily Safra Children Hospital, Sheba Medical Center, Tel-Hashomer 52621, Israel*

[c]*Department of Molecular Genetics and Biochemistry, Faculty of Medicine, Tel Aviv University, Tel Aviv, Israel*

[d]*The Wolfson Centre for Applied Structural Biology, Hebrew University of Jerusalem, Safra Campus, Givat Ram, Jerusalem 91904, Israel*

† Electronic supplementary information (ESI) available. See DOI: 10.1039/c6sc00115g

disordered region, like STIL.[21,29] Here we show that STIL contains two Zn^{2+} binding sites: the structured N terminal domain (NTD) and the intrinsically disordered region (IDR). Binding of Zn^{2+} ions had two parallel and different effects on the two domains: it induced structural changes in the NTD and oligomerization of the IDR. The oligomerization was critical for the interaction of STIL with its partner proteins. We conclude that the presence of a disordered and a structured domain in the same protein is essential for achieving two outcomes, structural changes and oligomerization, by binding the same metal ion.

Results

Structural characterization of STIL NTD and IDR

The N terminal domain of STIL (residues 2–370) and the central region of STIL (residues 450–700) were expressed and purified as HLT-fusion recombinant proteins.[24] The structural properties of these two fragments were studied using SEC and CD spectroscopy. We have previously shown that HLT STIL 450–700 is intrinsically disordered[24] and exists in an equilibrium between high and low oligomeric states (Fig. S1†). HLT STIL NTD, which is predicted to be fully structured,[24] eluted in SEC as a monomer as confirmed by SEC-MALS experiments (Fig. 1B). CD experiments showed that HLT STIL NTD is composed of secondary structure elements and lacks disordered conformations (Fig. 1C). Taken together, our results provide experimental evidence that STIL NTD is a structured monomer while STIL 450–700 is disordered.

Both STIL NTD and IDR bind Zn^{2+} ions

The amino acid composition of STIL contains a high percentage of negatively charged residues (Glu and Asp), which are common in disordered proteins and are known to participate in metal ion binding.[30,31] STIL also has a relatively high proportion of Cys and His residues, known to participate in metal ion binding,[31] similar to Zn^{2+} binding proteins (Fig. S2†). Since both Cys and His are common ligands of soft metal ions, we tested the possibility that STIL is a Zn^{2+} binding protein. STIL may be already bound to Zn^{2+} ions following its expression and thus we performed atomic absorption (AA) spectroscopy on HLT STIL NTD and HLT STIL IDR to detect the possible presence of the metal ions (Table 1). The results suggest a binding stoichiometry of 1 : 1 between HLT STIL NTD and Zn^{2+} as well as between the multimeric HLT STIL IDR and Zn^{2+}. The zinc absorbance in the sample of monomeric STIL IDR was at the sensitivity limit of the instrument and therefore we concluded that the HLT STIL IDR monomer was not pre-bound to Zn^{2+} ions while the multimeric HLT STIL IDR and HLT STIL NTD were pre-bound to Zn^{2+} ions. The AA results combined with the SEC results (Fig. S1†) indicate that HLT STIL IDR exists in an equilibrium between a monomer that is unbound to Zn^{2+} ions and a Zn^{2+} pre-bound multimer. Thus, the IDR was studied in its monomeric and multimeric forms. AA studies showed no presence of other metal ions, including Fe^{2+}, Ni^{2+}, Cu^{2+} or Ca^{2+} in the protein samples. Zn^{2+} or Ni^{2+} ions that may be bound by the His-tag during the purification process were not detected in the sample of HLT alone. In the case of HLT STIL NTD, addition of Zn^{2+} ions was significantly important to prevent protein precipitation during the expression (Fig. S3†), suggesting that Zn^{2+} is important for the correct folding of the protein.

To characterize the binding of Zn^{2+} ions to the STIL fragments, we used isothermal titration calorimetry (ITC). Since HLT STIL NTD and the multimeric HLT STIL IDR are already pre-bound to Zn^{2+} ions, we titrated EDTA into the protein to complex the Zn^{2+} ions. The addition of EDTA to HLT STIL NTD and to HLT STIL IDR resulted in the dissociation of Zn^{2+} ions from the proteins (Fig. 2A and B). Fitting the curves to one set of sites revealed a stoichiometry of 1 : 1 between EDTA and the

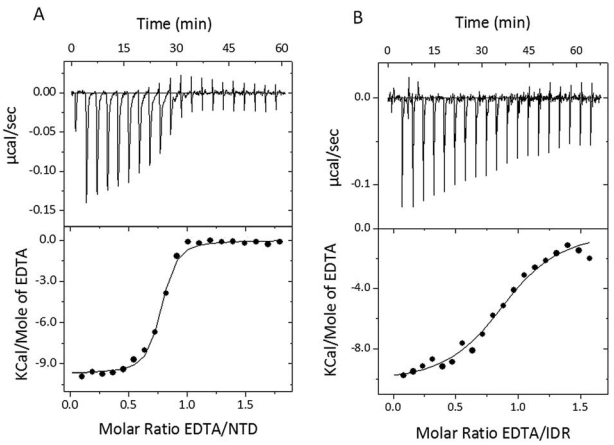

Fig. 2 STIL IDR and NTD are bound to Zn^{2+} ions. (A) ITC binding curve illustrating titration of EDTA into holo-HLT STIL NTD. (B) ITC binding curve illustrating titration of EDTA into multimeric HLT STIL IDR. The upper panels represent the baseline corrected raw data and the lower panels show the integrated curve fit to one set of sites.

Table 1 Zn^{2+} concentrations in STIL fragments as measured by atomic absorption[a]

STIL fragment	Protein concentration (µM)	AU	$[Zn^{2+}]$ (µM)
HLT STIL NTD	20	0.145 ± 0.001	18.5 ± 0.1
HLT STIL IDR multimer	6	0.023 ± 0.002	6.2 ± 0.7
HLT STIL IDR monomer	3	0.005 ± 0.001	—
HLT	6	Undetectable	—

[a] Solutions of HLT STIL NTD and multimeric or monomeric HLT STIL IDR were tested in an atomic absorption spectrophotometer (Perkin Elmer). The table presents the absorption of the Zn atom at 213.9 nm (AU) and the calculated concentrations of the Zn^{2+} ion in the protein samples.

proteins, which is equal to the EDTA : Zn^{2+} ratio (Table 2). Residual apo-STIL IDR or NTD that may exist in the samples would affect only the stoichiometry of the binding and not any of the thermodynamic parameters calculated from the ITC. We conclude that Zn^{2+} is bound to both the STIL NTD and IDR through one binding site in each domain. The thermodynamic parameters calculated from the fit are shown in Table 2 and represent the binding of EDTA to the Zn^{2+} ions that are released from the protein. While the changes in enthalpy and the changes in Gibbs free energy are very similar for the NTD and IDR, the changes in entropy (-2.6 cal mol^{-1} K^{-1} for the NTD and -8.67 cal mol^{-1} K^{-1} for the IDR) and the affinities were different (K_d of 0.12 ± 0.02 μM for the NTD and 0.8 ± 0.1 μM for the IDR). Titration of EDTA into free Zn^{2+} ions under the same experimental conditions revealed a K_d of 0.043 μM (data not shown). We calculated the K_d of Zn^{2+} binding to the STIL fragments using eqn (1)–(3) and found that the STIL NTD binds Zn^{2+} with a K_d of 0.36 μM and the STIL IDR binds Zn^{2+} with a K_d of 0.05 μM. This indicates that the STIL IDR binds Zn^{2+} 7 times more strongly than the STIL NTD. The higher change in entropy observed for the IDR may indicate that more significant conformational changes occur in the disordered STIL IDR compared to the structured STIL NTD. Other events coupled to the binding, such as proton exchange, may also contribute to this higher ΔS.

Structural changes of STIL NTD and IDR induced by Zn^{2+} binding

To study the possible conformational changes of the two STIL fragments upon Zn^{2+} binding we used limited proteolysis.[32,33] HLT STIL NTD was first treated with EDTA to generate the apo-protein. Apo-HLT STIL NTD and monomeric HLT STIL IDR were incubated with subtilisin, chymotrypsin or proteinase K, in the presence or absence of $ZnCl_2$ (Fig. 3). HLT STIL IDR was cleaved by most of the protease concentrations in the absence of $ZnCl_2$ but was not cleaved in the presence of $ZnCl_2$ (Fig. 3A and B). HLT STIL NTD was also cleaved by most of the protease concentrations in the absence of $ZnCl_2$ but was not cleaved at the lower protease concentrations in the presence of $ZnCl_2$ (Fig. 3C and D). $ZnCl_2$ had no effect on the digestion of ovalbumin, indicating that its presence does not directly affect the activity of the proteases (Fig. S4†). Overall, the results indicate that HLT STIL NTD and HLT STIL IDR acquire a conformation that is more resistant to proteases in the presence of Zn^{2+} ions. This shielded conformation can be due to structural changes to a more compact form or due to oligomerization of the protein. Tryptophan fluorescence spectra of the STIL NTD (containing four Trp residues) and the STIL IDR (containing one Trp residue) in the presence or absence of Zn^{2+} ions also reveal structural changes between the apo and holo proteins, which can be due to structural rearrangements or oligomerization (Fig. S5†).

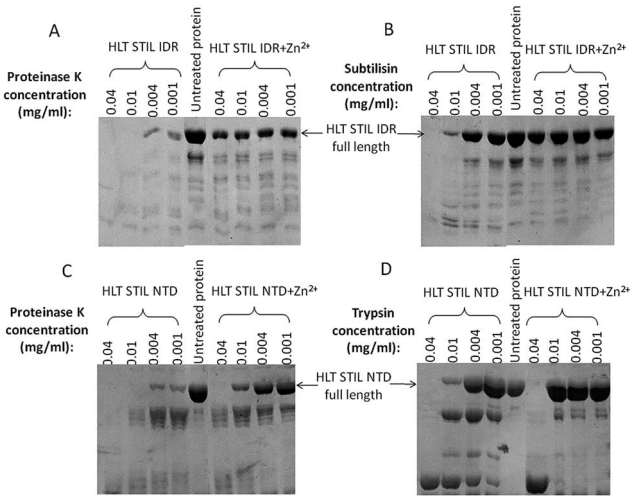

Fig. 3 Protease digestion of HLT STIL NTD and HLT STIL IDR: SDS-PAGE gel of HLT STIL IDR with and without $ZnCl_2$ at several concentrations of proteinase K (A) or subtilisin (B); SDS-PAGE gel of HLT STIL NTD with and without $ZnCl_2$ at several concentrations of proteinase K (C) or trypsin (D).

To follow possible structural changes caused by Zn^{2+} binding we used CD spectroscopy. The CD spectrum of HLT STIL NTD after EDTA addition shows a shift of the major peak from 210 nm towards 215 nm, representing the increase in the β sheet content after EDTA addition. This indicates a change in the secondary structure between the apo and the holo STIL NTD (Fig. 4A). A similar structural change was observed after heating the protein to 60 °C, which is an alternative way of releasing Zn^{2+} ions from the binding Cys residues due to oxidation of the thiols.[34] On the contrary, removal of Zn^{2+} ions did not change the secondary structure of the IDR fragment: the CD spectrum of the monomeric protein which was unbound to Zn^{2+} ions was similar to the CD spectrum of the Zn^{2+} pre-bound multimeric protein (Fig. 4B). Near-UV CD experiments also support structural changes in the STIL NTD in the presence of Zn^{2+} ions (Fig. S6†). Removing the Zn^{2+} ions by adding EDTA resulted in changes in the spectrum, mainly in the 270–280 nm region corresponding to the aromatic side chains. This reflects differences between the tertiary structures of the apo and holo STIL NTD.

Table 2 Thermodynamic parameters calculated from the ITC data[a]

Fragment	No. of sites	K_d (μM)	ΔH (kcal mol^{-1})	ΔS (cal mol^{-1} K^{-1})	ΔG (kcal mol^{-1})
NTD	0.74 ± 0.01	0.12 ± 0.02	-9.7 ± 0.1	-2.6	-9.0 ± 0.1
IDR	0.91 ± 0.02	0.8 ± 0.1	-10.3 ± 0.3	-8.67	-7.8 ± 0.3

[a] The thermodynamic parameters represent the binding of EDTA to Zn^{2+} ions in each experiment.

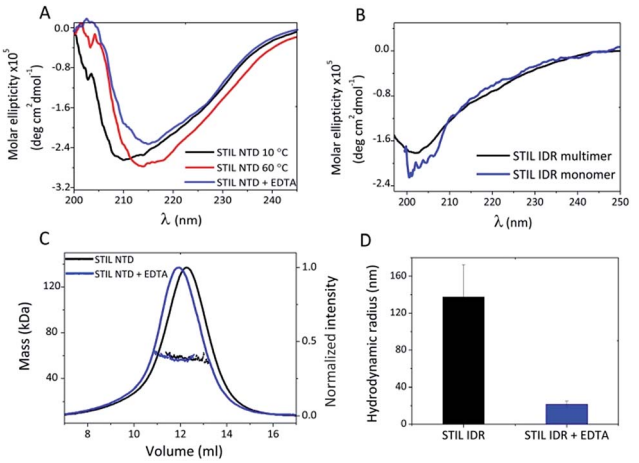

Fig. 4 Structural changes in STIL fragments induced by binding of Zn^{2+} ions: (A) CD spectra of HLT STIL NTD at 10 °C and at 60 °C and with addition of EDTA. (B) CD spectra of pre-bound Zn^{2+} multimeric HLT STIL IDR and Zn^{2+}-free monomeric HLT STIL IDR. (C) SEC MALS of HLT STIL NTD alone and with EDTA addition. (D) Hydrodynamic radius of multimeric HLT STIL IDR before and after EDTA addition, as measured using DLS.

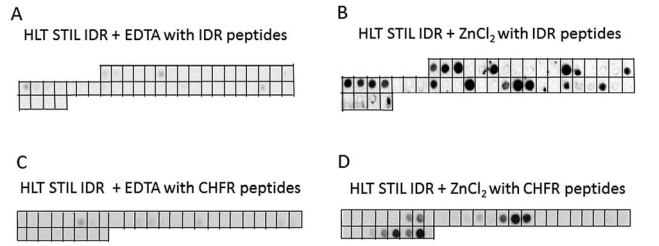

Fig. 5 Binding of the STIL IDR to STIL and CHFR derived peptide arrays: binding of HLT STIL IDR to an array of peptides derived from the STIL IDR in the presence of EDTA (A) or $ZnCl_2$ (B); binding of HLT STIL IDR to an array of CHFR derived peptides in the presence of EDTA (C) or $ZnCl_2$ (D). Each dark spot indicates binding between the STIL fragment and the corresponding peptide.

To study oligomerization changes that may be induced by Zn^{2+} binding we used static and dynamic light scattering. SEC-MALS measurements of HLT STIL NTD revealed that the observed mass of the protein before and after EDTA treatment was the same (58 ± 2 kDa), in agreement with the calculated mass of the monomer (55 kDa). This indicates that the STIL NTD is monomeric and oligomerization did not occur (Fig. 4C). The elution volume of HLT STIL NTD with EDTA was slightly lower than that of free STIL NTD, indicating a minor change in the structure of the protein to a more extended conformation. We conclude that Zn^{2+} binding induces structural changes in the STIL NTD to a more compact form. We used DLS to measure the hydrodynamic radius of multimeric STIL IDR (which is pre-bound to Zn^{2+} ions) before and after the addition of EDTA (Fig. 4D). A significant decrease in the radius of HLT STIL IDR after EDTA addition was observed, from a radius of 137 ± 35 nm of the oligomer to a radius of 22 ± 4 nm of the EDTA treated protein. We conclude that the presence of Zn^{2+} ions induces oligomerization of the STIL IDR. Taken together, our results indicate that binding of Zn^{2+} ions induces structural changes in the structured STIL NTD and oligomerization of the STIL IDR.

Identification of the oligomerization sites within STIL IDR

To characterize the oligomerization sites within the STIL IDR, we used peptide array screening. We designed an array of partly overlapping peptides derived from the STIL IDR (residues 370–700) and screened it for binding HLT STIL IDR itself in the presence of $ZnCl_2$ or EDTA. HLT STIL IDR bound several peptides derived from the STIL IDR only in the presence of $ZnCl_2$, while it did not bind the peptides in the presence of EDTA (Fig. 5A and B). The binding peptides may represent the oligomerization sites within the STIL IDR (Fig. S7†) or indicate intramolecular interactions within this domain. Most of the binding peptides contain a high proportion of Zn^{2+} binding residues (Cys, His, Glu or Asp), as detailed in ESI Table S1.† This observation further supports our conclusion that Zn^{2+} ions mediate STIL oligomerization. Alignment of the peptide sequences did not reveal known binding motifs. However, using the Block Maker tool[35] we identified a new motif of 5 residues in most of the sequences. This motif contains Ser residues at the termini and a positive residue (His or Lys) or Leu residue in the middle: SxKxS/SxHxS or SxLxS (Table S1†). This motif as well as the Zn^{2+} binding residues are spread throughout the entire IDR sequence (Fig. S8†). HLT STIL NTD did not bind any peptides on an array derived from the STIL NTD, supporting the finding that this domain does not oligomerize (Fig. S9A and B†).

Oligomerization of STIL IDR is required for the interaction with CHFR

We tested whether the Zn^{2+} binding is required for the interactions of STIL with its partner proteins, using the tumor suppressor CHFR as a model.[24] An array of partly overlapping peptides derived from CHFR was designed and screened for binding with HLT STIL IDR and HLT STIL NTD in the presence of $ZnCl_2$ or EDTA (Fig. 5C and D, S9C and S9D†). The results show that while the STIL IDR mediates the interaction of the protein with the CHFR peptides, the NTD does not bind CHFR peptides. Binding of HLT STIL IDR to the peptides was detected in the presence of Zn^{2+} ions while in the presence of EDTA almost no binding was observed. We conclude that oligomerization of STIL, induced by Zn^{2+} ions, is crucial for the STIL–CHFR interaction. The oligomerization may mediate the interaction with CHFR or other target proteins by exposing specific motifs required for the interaction. The Zn^{2+} ions may also serve as a direct mediator of the interaction between the STIL and CHFR peptides. It could be that both mechanisms take place in parallel. The HLT alone did not bind the peptide arrays in the presence of $ZnCl_2$ (Fig. S9E and F†).

Discussion

Zn^{2+} binding to disordered regions was shown to induce a disorder to order transition and gain of structure in many cases[36–38] or lead to oligomerization, mainly aggregation, of

IDPs.[11,12,39] Here we show that binding of Zn^{2+} ions induces different effects on structured and disordered domains in the same protein: while binding of Zn^{2+} induced structural changes in the structured STIL NTD, it did not induce structural rearrangement or gain of structure of the disordered domain of STIL. Rather, it led to oligomerization of the disordered domain. The disordered region preserves its disordered features upon binding the Zn^{2+} ion ligand and oligomerizes to form an active protein. This oligomerization is reversible, as shown by the DLS studies (Fig. 4D) and may be a part of the regulation of the full length protein. Since the oligomerization of the STIL IDR is critical for its protein interactions, it may mediate the interaction with the target proteins by exposing specific motifs required for the interaction. Many centrosomal proteins act as oligomeric complexes that are crucial for centrosomal processes and functions.[20,40,41] STIL may also act as an oligomeric complex in the centriole. Binding of Zn^{2+} ions can be one of the mechanisms to control its oligomerization.

The STIL IDR oligomerization sites, as revealed by the peptide array screening, contain a high proportion of Zn^{2+} binding residues, Cys and His, at different positions in the IDR sequence (Fig. S8†). These together create the binding site of the Zn^{2+} ion. The Zn^{2+} binding site may be composed of residues from different IDR domains that are sequentially distant. Using this mechanism Zn^{2+} binding can bring these regions close together and, if they are from different monomers, directly mediate the oligomerization. Since the STIL IDR binds Zn^{2+} ions in a stoichiometry of 1 : 1 (Table 1), it is likely that not all of the Cys and His residues participate in the Zn^{2+} binding. In addition, alignment of the peptide sequences revealed a new suggested motif for oligomerization: SxKxS/SxHxS or SxLxS (Table S1†). This motif resembles the SxxxS phosphorylation motif[42] although here we used non-phosphorylated proteins or peptides. Since the STIL IDR contains several phosphorylation sites that mediate interactions of STIL,[25] phosphorylation together with the oligomerization may play a part in the regulation of the protein. Binding of Zn^{2+} ions may induce conformational rearrangement of the STIL IDR, leading to exposure of this motif and enabling the oligomerization. The binding affinity of the STIL NTD and STIL IDR to Zn^{2+} ions, as revealed by the ITC experiments, is relatively strong compared to the binding affinities of Zn^{2+} ions to other Zn^{2+}-binding proteins. Zn^{2+} binding to other proteins has a range of K_d between submicromolar to micromolar. BSA binds Zn^{2+} with a K_d of 1 μM,[43] p25 binds Zn^{2+} with a K_d of 30 μM,[9] α-crystallin binds Zn^{2+} ions with a K_d of 100 μM[5] and the S100B protein binds Zn^{2+} with a K_d of 94 nM.[44]

The binding of Zn^{2+} ions to the STIL IDR (K_d = 50 nM) was stronger than the binding of Zn^{2+} ions to the STIL NTD (K_d = 360 nM). This emphasizes the significance of Zn^{2+} ions in this region and highlights the generally important role that the IDR plays in the protein. The binding of the same metal ion through a disordered and a structured domain in the same protein is a property that may have implications in regulating the activity of the protein. By doing so, the protein achieves two parallel outcomes: structural changes and oligomerization that can take place together (Fig. 6).

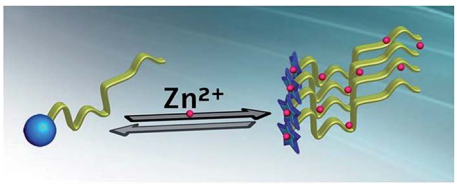

Fig. 6 A proposed mechanism for binding of Zn^{2+} ions to STIL: binding of Zn^{2+} ions induces structural changes in the STIL NTD (the blue circle changes into a star) and oligomerization of the STIL IDR (yellow ribbon) in parallel and allows protein activity.

Experimental

Expression and purification of the STIL domains

Preparation of DNA encoding fragments of STIL was performed as detailed before.[24] The proteins were expressed fused to the HLT tag that contains six His residues, a Lipo-domain for enhanced solubility and a Tev protease cleavage site for removing the tag (Fig. S10†). HLT STIL 2–370 (NTD) and HLT STIL 450–700 (IDR) vectors were transformed into *E. coli* BL21(DE3) pLysS cells (Novagen). Expression and purification of HLT STIL IDR were performed as previously described.[24] HLT STIL NTD transformed bacteria cells were grown at 37 °C in 2xYT medium. At an $OD_{600\ nm}$ of 0.2 heat-shock treatment was performed by adding 0.1% glycerol and 0.1 mM potassium glutamate and the bacteria were incubated at 42 °C for 20 min. The temperature was reduced to 37 °C and the bacteria were grown until an $OD_{600\ nm}$ of 0.7. 0.1 mM $ZnCl_2$ and 0.1 mM IPTG were added to start the induction that was carried out overnight at 22 °C. The bacteria were harvested, sedimented as pellets and kept at −80 °C. The bacteria were lysed using a microfluidizer and the soluble fraction was purified using a nickel Sepharose column. Elution was performed using an imidazole gradient and the protein was eluted with 25 mM TrisHCl buffer, pH = 8.5, 0.5 M NaCl, 5 mM βMe, 10% glycerol and 250 mM imidazole. The eluted protein was further purified using size exclusion chromatography with a Sephacryl S100 500 ml column. Elution was performed with a buffer of 25 mM Hepes, pH = 7, 0.3 M NaCl, 5 mM βMe and 2% glycerol. This buffer was also used as the storage buffer. The protein purity was confirmed by Coomassie staining of an SDS-PAGE gel.

SEC and SEC-MALS

45 μM HLT STIL NTD was dissolved in 20 mM Hepes buffer, pH = 7, 150 mM NaCl, 2% glycerol and 2 mM βMe and was loaded on a Superose12 analytical GF column. A Multi Angle Light Scattering (MALS) miniDAWN TREOS instrument of Wyatt technology was used to measure the molecular weight of the protein alone and after 10 mM EDTA addition and 4 hours of incubation on ice. HLT STIL IDR was loaded on a Superose12 analytical GF column and eluted with 20 mM Hepes buffer, pH = 7, 300 mM NaCl, 2% glycerol and 2 mM βMe.

Isothermal titration calorimetry (ITC)

ITC measurements were carried out at 10 °C on an isothermal titration calorimeter (ITC 200, MicroCal). 23 μM HLT STIL NTD

and 13 μM HLT STIL IDR were dissolved in 13 mM Hepes buffer, pH = 7, 150 mM NaCl, 2% glycerol and 2 mM βMe. 100–200 μM EDTA was dissolved in the same buffer and titrated into the protein samples. 2 μl of EDTA solution was injected into the protein sample in 2 s titrations. A 180 s delay between injections was allowed for equilibration.[45] Titration of EDTA into the buffer solution, titration of EDTA into the HLT solution and titration of the buffer into the protein solutions were performed as controls. The ITC data were analyzed with Origin 7.0 software.

K_d of Zn^{2+}–EDTA binding in a free Zn^{2+} solution was measured using ITC and is described by equation (1):

$$K_d{}^1 = \frac{[EDTA][Zn^{2+}]}{[(EDTA - Zn^{2+})]} \quad (1)$$

K_d of Zn^{2+}–EDTA binding in the STIL fragment solution was measured by ITC and is described by equation (2):

$$K_d{}^2 = \frac{[EDTA][(STIL - Zn^{2+})]}{[(EDTA - Zn^{2+})][STIL]} \quad (2)$$

The K_d of Zn^{2+}–STIL fragment binding was calculated using eqn (3):

$$K_d{}^3 = \frac{K_d{}^1}{K_d{}^2} = \frac{[Zn^{2+}][STIL]}{[(STIL - Zn^{2+})]} \quad (3)$$

These calculations are under the assumption that EDTA binds only Zn^{2+} and not the protein and that STIL binds Zn^{2+} in a stoichiometry of 1 : 1.

Atomic absorption spectroscopy

HLT STIL NTD, HLT STIL IDR multimeric fraction and monomeric fraction, and HLT samples were analyzed in an atomic absorption spectrophotometer 3110 or AAnalyst 400 (Perkin Elmer), with a Zn lamp at a wavelength of 213.9 nm. Samples were dissolved in 25 mM Hepes, pH = 7, 300 mM NaCl, 2 mM βMe and 2% glycerol.

Circular dichroism (CD)

CD spectra of HLT STIL NTD and HLT STIL IDR were recorded using a J-810 spectropolarimeter (Jasco) in a 0.1 cm quartz cuvette for far-UV CD spectroscopy, in a spectral range of 195 nm to 260 nm. 16 μM HLT STIL NTD was incubated with 10 mM EDTA for 8 hours on ice, then dialyzed using 15 mM Hepes buffer, pH = 7, 150 mM NaCl, 2 mM βMe and 2% glycerol. CD spectra were recorded at 10 °C for 10 μM protein without EDTA addition and for the sample after EDTA treatment. A CD spectrum was also recorded for 10 μM protein at 60 °C. 3 μM monomeric HLT STIL IDR was dissolved in PBS buffer containing 2% glycerol and 2 mM βMe, and CD spectra of the protein alone and with the addition of $ZnCl_2$ were recorded. A CD spectrum of 3 μM multimeric HLT STIL IDR dissolved in 20 mM TrisHCL, pH = 7.5, 50 mM Na_2SO_4, 0.5 mM βMe and 2% glycerol was also recorded. Near-UV CD spectra, in a spectral range of 250 nm to 340 nm, were recorded for 145 μM HLT STIL NTD alone or with addition of 10 mM EDTA. The measurements were performed in 25 mM Hepes buffer, pH = 7, 300 mM NaCl, 5 mM βMe and 5% glycerol.

Dynamic light scattering (DLS)

Multimeric HLT STIL IDR was incubated with 10 mM EDTA for 2 days at 4 °C. DLS measurements were performed using a Zetasizer Nano-ZS (Malvern instruments) at 10 °C and the average hydrodynamic radius was calculated by the intensity for the protein alone and with EDTA addition. The calculation was performed using the Stokes–Einstein equation:

$$R_H = kT/6\pi\eta D,$$

where R_H is the hydrodynamic radius, k is Boltzmann's constant, T is the temperature, η is the viscosity of the sample and D is the translational diffusion coefficient.[46] The calculated radius is based on the assumption that the particles are spherical.

Partially limited proteolysis

20 μl of 20 μM HLT STIL NTD was incubated with 10 mM EDTA for 5 hours on ice followed by overnight dialysis in 20 mM Hepes buffer, pH = 7, 150 mM NaCl, 2 mM βMe and 2% glycerol to remove the EDTA excess. 20 μl of 9 μM monomeric HLT STIL IDR was dissolved in 20 mM Hepes buffer, pH = 7, 300 mM NaCl, 2 mM βMe and 2% glycerol. The proteins were incubated with 5 μl of subtilisin, chymotrypsin or proteinase K at increasing concentrations with the presence or absence of 0.3 mM $ZnCl_2$. After 30 min at 22 °C the proteolytic reaction was stopped by adding 6.5 μl of SDS solution, 5.2 mM PMSF and 5.2 mM EDTA. Ovalbumin was also treated with the above proteases in the presence or absence of 0.3 mM $ZnCl_2$, as a control for ensuring that Zn^{2+} ions do not affect the activity of the proteases. The cleaved products were run on 12% SDS-PAGE gels.

Fluorescence spectroscopy

Tryptophan fluorescence spectra were recorded using an LS45 luminescence spectrophotometer (Perkin Elmer). 2.5 μM monomeric HLT STIL IDR and 2.5 μM multimeric HLT STIL IDR were dissolved in 25 mM Hepes buffer, pH = 7, 150 mM NaCl, 2% glycerol and 2 mM βMe. Excitation was performed at 280 nm and the emission was screened between 300 nm to 430 nm. 0.25 μM HLT STIL NTD was dissolved in the same buffer and fluorescence measurements were performed using the same settings for the NTD sample alone and with addition of 10 mM EDTA.

Peptide array screening

An array of 94 partly overlapping STIL derived peptides and an array of 32 partly overlapping CHFR derived peptides were synthesized by INTAVIS Bioanalytical Instruments AG, Koeln, Germany. The peptides were acetylated at their N-termini and attached to a cellulose membrane *via* their C-termini through an amide bond. The arrays were washed with TBST (50 mM

TrisHCl, pH = 7.5, 150 mM NaCl, 0.1% Tween20) containing 2.5% milk. 3–5 μM HLT STIL NTD and monomeric HLT STIL IDR were dissolved in TrisHCl buffer, pH = 7.5, 150 mM NaCl, 5 mM βMe, 2% glycerol, 0.1% Tween20 and 2.5% milk, in the presence of 0.3 mM $ZnCl_2$ or 10 mM EDTA, and incubated with the arrays at 4 °C with shaking overnight. After washing with TBST in the presence of 0.3 mM $ZnCl_2$ or 10 mM EDTA, the arrays were incubated with an anti-His HRP conjugated antibody at room temperature for 1 hour and then washed again with TBST. Immunodetection was performed using chemiluminescence with ECL reagents.

Acknowledgements

AF is supported by grants from the Israel Science Foundation (ISF), the Israel Cancer Research Foundation (ICRF) and by the Minerva Centre for Bio-Hybrid Complex Systems. HA is supported by the Dalia and Dan Meydan fellowship for Ph.D. students. AD is supported by an Eshkol grant from the Israel Science Ministry. SI is supported by grants from the Israel Science Foundation and Israel Science Ministry.

References

1 X. Arias-Moreno, O. Abian, S. Vega, J. Sancho and A. Velazquez-Campoy, *Curr. Protein Pept. Sci.*, 2011, **12**, 325–338.
2 H. S. Won, L. Y. Low, R. De Guzman, M. Martinez-Yamout, U. Jakob and H. Jane Dyson, *J. Mol. Biol.*, 2004, **341**, 893–899.
3 T. Yu, G. Wu, H. Yang, J. Wang and S. Yu, *Int. J. Biol. Macromol.*, 2013, **56**, 57–61.
4 M. Tourbez, C. Firanescu, A. Yang, L. Unipan, P. Duchambon, Y. Blouquit and C. T. Craescu, *J. Biol. Chem.*, 2004, **279**, 47672–47680.
5 S. Karmakar and K. P. Das, *Biopolymers*, 2011, **95**, 105–116.
6 M. C. Mayer, D. Kaden, L. Schauenburg, M. A. Hancock, P. Voigt, D. Roeser, C. Barucker, M. E. Than, M. Schaefer and G. Multhaup, *J. Biol. Chem.*, 2014, **289**, 19019–19030.
7 A. Chenal, J. C. Karst, A. C. Sotomayor Pérez, A. K. Wozniak, B. Baron, P. England and D. Ladant, *Biophys. J.*, 2010, **99**, 3744–3753.
8 N. Selevsek, S. Rival, A. Tholey, E. Heinzle, U. Heinz, L. Hemmingsen and H. W. Adolph, *J. Biol. Chem.*, 2009, **284**, 16419–16431.
9 A. Zotter, J. Olah, E. Hlavanda, A. Bodor, A. Perczel, K. Szigeti, J. Fidy and J. Ovadi, *Biochemistry*, 2011, **50**, 9568–9578.
10 A. C. Sotomayor-Pérez, D. Ladant and A. Chenal, *J. Biol. Chem.*, 2011, **286**, 16997–17004.
11 T. Bund, J. M. Boggs, G. Harauz, N. Hellmann and D. Hinderberger, *Biophys. J.*, 2010, **99**, 3020–3028.
12 R.-H. Li, G.-B. Liu, H. Wang and Y.-Z. Zheng, *Biosci., Biotechnol., Biochem.*, 2013, **77**, 475–481.
13 P. D. Aplan, D. P. Lombardi and I. R. Kirsch, *Mol. Cell. Biol.*, 1991, **11**, 5462–5469.
14 A. Erez, A. Castiel, L. Trakhtenbrot, M. Perelman, E. Rosenthal, I. Goldstein, N. Stettner, A. Harmelin, H. Eldar-Finkelman, S. Campaner, I. Kirsch and S. Izraeli, *Cancer Res.*, 2007, **67**, 4022–4027.
15 S. Izraeli, L. A. Lowe, V. L. Bertness, D. J. Good, D. W. Dorward, I. R. Kirsch and M. R. Kuehn, *Nature*, 1999, **399**, 691–694.
16 K. L. Pfaff, C. T. Straub, K. Chiang, D. M. Bear, Y. Zhou and L. I. Zon, *Mol. Cell. Biol.*, 2007, **27**, 5887–5897.
17 J. Vulprecht, A. David, A. Tibelius, A. Castiel, G. Konotop, F. Liu, F. Bestvater, M. S. Raab, H. Zentgraf, S. Izraeli and A. Krämer, *J. Cell Sci.*, 2012, **125**, 1353–1362.
18 C. Arquint, K. F. Sonnen, Y.-D. Stierhof and E. A. Nigg, *J. Cell Sci.*, 2012, **125**, 1342–1352.
19 A. Castiel, M. M. Danieli, A. David, S. Moshkovitz, P. D. Aplan, I. R. Kirsch, M. Brandeis, A. Kramer and S. Izraeli, *J. Cell Sci.*, 2011, **124**, 532–539.
20 R. Qiao, G. Cabral, M. M. Lettman, A. Dammermann and G. Dong, *EMBO J.*, 2012, **31**, 4334–4347.
21 M. A. Cottee, N. Muschalik, S. Johnson, J. Leveson, J. W. Raff and S. M. Lea, *eLife*, 2015, **4**, e07236.
22 S. Ramaswamy, K. N. Ross, E. S. Lander and T. R. Golub, *Nat. Genet.*, 2003, **33**, 49–54.
23 A. Kumar, S. C. Girimaji, M. R. Duvvari and S. H. Blanton, *Am. J. Hum. Genet.*, 2009, **84**, 286–290.
24 H. Amartely, A. David, M. Lebendiker, H. Benyamini, S. Izraeli and A. Friedler, *Chem. Commun.*, 2014, **50**, 5245–5247.
25 S. Campaner, P. Kaldis, S. Izraeli and I. R. Kirsch, *Mol. Cell. Biol.*, 2005, **25**, 6660–6672.
26 C. J. Tang, S. Y. Lin, W. B. Hsu, Y. N. Lin, C. T. Wu, Y. C. Lin, C. W. Chang, K. S. Wu and T. K. Tang, *EMBO J.*, 2011, **30**, 4790–4804.
27 N. R. Stevens, J. Dobbelaere, K. Brunk, A. Franz and J. W. Raff, *J. Cell Biol.*, 2010, **188**, 313–323.
28 C. Arquint, A.-M. Gabryjonczyk, S. Imseng, R. Böhm, E. Sauer, S. Hiller, E. A. Nigg and T. Maier, *eLife*, 2015, **4**, e07888.
29 E. Shimanovskaya, R. Qiao, J. Lesigang and G. Dong, *Worm*, 2013, **2**, e25214.
30 V. N. Uversky and A. K. Dunker, *Biochim. Biophys. Acta*, 2010, **1804**, 1231–1264.
31 B. L. Vallee and D. S. Auld, *Biochemistry*, 1990, **29**, 5647–5659.
32 A. Fontana, P. Polverino de Laureto, V. De Filippis, E. Scaramella and M. Zambonin, *Folding Des.*, 1997, **2**, R17–R26.
33 T. Moldoveanu, C. M. Hosfield, Z. Jia, J. S. Elce and P. L. Davies, *Biochim. Biophys. Acta*, 2001, **1545**, 245–254.
34 U. Jakob, M. Eser and J. C. A. Bardwell, *J. Biol. Chem.*, 2000, **275**, 38302–38310.
35 S. Henikoff, S. Pietrokovski and J. G. Henikoff, *Nucleic Acids Res.*, 1998, **26**, 309–312.
36 F. Guillière, C. Danioux, C. Jaubert, N. Desnoues, M. Delepierre, D. Prangishvili, G. Sezonov and J. I. Guijarro, *PLoS One*, 2013, **8**, e52908.
37 K. Banaszak, V. Martin-Diaconescu, M. Bellucci, B. Zambelli, W. Rypniewski, M. J. Maroney and S. Ciurli, *Biochem. J.*, 2012, **441**, 1017–1026.

38 L. Rahman, V. Bamm, J. M. Voyer, G. T. Smith, L. Chen, M. Yaish, B. Moffatt, J. Dutcher and G. Harauz, *Amino Acids*, 2011, **40**, 1485–1502.
39 P. Faller, C. Hureau and G. La Penna, *Acc. Chem. Res.*, 2014, **47**, 2252–2259.
40 G. Lukinavičius, D. Lavogina, M. Orpinell, K. Umezawa, L. Reymond, N. Garin, P. Gönczy and K. Johnsson, *Curr. Biol.*, 2013, **23**, 265–270.
41 K. Habermann and B. M. Lange, *Cell Div.*, 2012, **7**, 17.
42 S.-Y. Lu, Y.-J. Jiang, J.-W. Zou and T.-X. Wu, *J. Chem. Inf. Model.*, 2011, **51**, 1025–1036.
43 J. Lu, A. J. Stewart, P. J. Sadler, T. J. T. Pinheiro and C. A. Blindauer, *Biochem. Soc. Trans.*, 2008, **36**, 1317–1321.
44 P. T. Wilder, D. M. Baldisseri, R. Udan, K. M. Vallely and D. J. Weber, *Biochemistry*, 2003, **42**, 13410–13421.
45 M. J. Cliff and J. E. Ladbury, *J. Mol. Recognit.*, 2003, **16**, 383–391.
46 A. Labrie, A. Marshall, H. Bedi and E. Maurer-Spurej, *Transfus. Med. Hemother.*, 2013, **40**, 93–100.